Coordinated Control of SVS and CSC for Damping Power System Oscillations

P. R. Sharma

Department of Electrical & Electronics Engineering
YMCA University of Science & Technology, Faridabad, India
prsharma1966@gmail.com

Abstract: In this paper the effectiveness of Static Var System (SVS) auxiliary controller in coordination with controlled series compensation has been demonstrated for damping power oscillations for wide range of operating conditions. A new SVS auxiliary controller, known as the combined derivative of reactive power and derivative of computed internal voltage (CDRPDCIV) auxiliary controller has been developed and incorporated in the SVS control system located at the middle of a series compensated long transmission line to get most effective damping effect. The first IEEE benchmark model for analysis of torsional modes has been adopted. Eigen value analysis study is conducted for various levels of power transfer and series compensation. The results of eigen value analysis are validated by carrying out time domain analysis study based on non linear model. The proposed SVS auxiliary controller in coordination with CSC with its bang – bang form of control is very effective in damping power system oscillations over a wide operating range under large disturbance conditions thus enhancing the Transient performance of the power system.
Keywords: Static Var System, Series compensation, Auxiliary controller, Torsional oscillations, Controlled series compensation

1. Introduction

Damping of power oscillations associated with the generator rotor swings is an important and challenging task in the power industry. These low frequency oscillations arise due to the dynamics of inter area power transfer and exhibit poor damping at high power transfer levels. Oscillations associated with single generator (Local Modes) have frequencies in the range of 0.8-1.8 Hz. The inter area modes have the frequency of oscillations in the range 0.2-0.5 Hz and involve large group of generators swinging against each other. The stability of these low frequency oscillations is a pre requisite for secure operation of system after critical contingencies.

With the advent of fast acting, power electronic based FACTS controllers like SVS, TCSC, SSSC, STATCOM, TCPAR and UPFC, it is feasible to enhance the damping of power system oscillations effectively at low cost [4, 5, 7, 11]. In recent years SVS has been employed to an increasing extent in modern power systems [1, 4, 10] due to its capability to work as Var generation and absorption systems. Besides, voltage control and improvement of transmission capability SVS in coordination with auxiliary controllers [3, 4, 6, 10] can be used for damping of power system oscillations. Damping of power system oscillations plays an important role not only in increasing the transmission capability but also for stabilization of power system conditions after critical faults, particularly in weakly coupled networks.

The controlled series compensation is one of the novel technique under FACTS philosophy for damping of power system oscillations [5]. D. Povh and Mihalic proposed the application of CSC and SVC for transient stability enhancement of an ac transmission system. Noroozian, M et. al. [6] proposed a robust control strategy for thyristor controlled series capacitor and static VAr systems to damp electromechanical oscillations. Larsen et al [2] have presented the design

Received: February 26, 2010. Accepted: May 19, 2010

concepts and a systemic approach for the selection of input signals for FACTS damping controllers based on various damping controller design indices. The angular difference of two remote voltages on each side of TCSC is chosen as damping controller input Control strategies for damping of electromechanical power oscillations using an energy function method have been proposed by Gronquist et al in [3], Chaudhuri, B. Pal et al designed a multiple –input Single output (MISO) controller for TCSC to improve damping of critical inter area modes using global stabilizing signals[12]. J. Chen et al proposed an equivalent model to analyse the capabilities of series connected FACTS controllers to damp power system oscillations and developed a universal control strategy using fuzzy logic control based on a locally measurable signal to enhance power system damping [11]. R.K.Verma [16] et.al. have described the use of TCSC for damping subsynchronous oscillations when provided with close loop current control. Alberto Mota Simoes [17] et.al. have proposed a power oscillation damping controller design implemented in TCSC to suppress low frequency oscillations. S.K.Gupta and N.Kumar proposed the application of CSC in coordination with double order SVS auxillary controller and induction machine for suppressing the torsional oscillations [15]. The control of the scheme is complex.

In the present literature it is seen that the system dynamics has not been properly taken into account as a result the models are less sensitive towards the voltage overshoots due to fast switching of controlled capacitors.

In the present paper the CDRPDCIV SVS auxiliary controller has been employed in coordination with controlled series compensation in a long series compensated transmission line A continuous control of mid point located SVS with the bang –bang form of control of CSC is very effective in damping Torsional oscillations. The above coordination provides an efficient and robust control of power oscillations damping for wide range of power transfer under large disturbance conditions.

2. System Model

The system investigated for this paper is well known IEEE first benchmark model depicted in Figure.1. System consist of 1110 MVA synchronous generator supplying power to an infinite bus over a 400 KV, 600Km long series compensated single circuit transmission line. The rotor shaft model of the system is a six spring mass model consist of six turbine sections which have been modeled separately: (a) high pressure stage (HP), an intermediate stage (IP), two low pressure stages (LP_A and LP_B), generator and excitor. The series compensation has been provided at the sending end of line. IEEE type1 excitation system is used for the generator. An SVS of switched capacitor and thyristor controlled reactor type is considered located at the middle of the transmission line which provides continuously controllable reactive power at its terminals in response to bus voltage and of derivative of computed internal voltage and derivative of reactive power auxiliary control signals. The system data and tortional spring mass system data are given in appendix A.

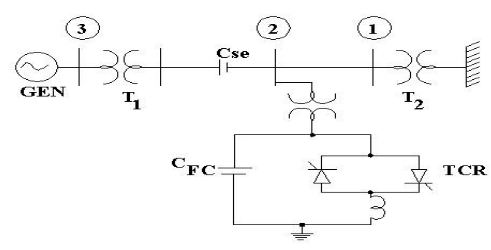

Figure 1. Electrical Network with SVS

A. Generator

In the detailed machine model [9] used here, the stator is represented by a dependent current source parallel with the inductance. The generator model includes the field winding 'f' and a damper winding 'h' along d-axis and two damper windings 'g' and 'k'along q-axis. The IEEE type-1 excitation system is used for the generator. In the mechanical model detailed shaft torque dynamics [2] has been considered for the analysis of torsional modes due to SSR.

$$\begin{aligned}\dot{\psi}_f &= a_1\psi_f + a_2\psi_h + b_1 v_f + b_2 i_d\\ \dot{\psi}_h &= a_3\psi_f + a_4\psi_h + b_3 i_d\\ \dot{\psi}_g &= a_5\psi_g + a_6\psi_k + b_5 i_q\\ \dot{\psi}_k &= a_7\psi_g + a_8\psi_k + b_6 i_q\end{aligned} \tag{1}$$

Where v_f is the field excitation voltage. Constants a_1 to a_8 and $b_1$to b_6 are defined in [10]. $i_{d,}$ i_q are d, and q axis components of the machine terminal current respectively which are defined with respect to machine reference frame. To have a common axis of representation with the network and SVS, these flux linkages are transformed to the synchronously rotating D-Q frame of reference using the following transformation:

$$\begin{bmatrix} i_d \\ i_q \end{bmatrix} = \begin{bmatrix} \cos\delta & -\sin\delta \\ \sin\delta & \cos\delta \end{bmatrix} \begin{bmatrix} i_D \\ i_Q \end{bmatrix} \tag{2}$$

Where $i_{D,}$ i_Q are the respective machine current components along D and Q axis. δ is the angle by which d-axis leads the D-axis. Currents I_d and $I_{q,}$ which are the components of the dependent current source along d
and q axis respectively, are expressed as:

$$\begin{aligned} I_d &= c_1\psi_f + c_2\psi_h\\ I_q &= c_3\psi_g + c_4\psi_k \end{aligned} \tag{3}$$

Where constants c_1- c_4 are defined in [14]. Substituting eqn. (2) in eqn. (1) and Linearizing gives the state and output equation of the rotor circuit as:

$$\begin{aligned} \dot{X}_R &= A_R X_R + B_{R1}U_{R1} + B_{R2}U_{R2} + B_{R3}U_{R3}\\ Y_{R1} &= C_{R1}X_R + D_{R1}U_{R1}\\ Y_{R2} &= C_{R2}X_R + D_{R2}U_{R1} + D_{R3}U_{R2} + D_{R4}U_{R3} \end{aligned} \tag{4}$$

where $X_R = \left[\Delta\psi_f \quad \Delta\psi_h \quad \Delta\psi_g \quad \psi_k\right]^t$, $U_{R1} = \left[\Delta\delta \quad \Delta\omega\right]^t$,

$U_{R2} = \Delta V_f$, $U_{R3} = \left[\Delta i_D \quad \Delta i_Q\right]^t$ $Y_{R1} = [\Delta I_D \quad \Delta I_Q]^t$

$Y_{R1} = [\Delta\dot{I}_D \quad \Delta\dot{I}_Q]^t$

B. Mechanical System

The mechanical system (Figure 2) is described by the six spring mass model. The governing equations and the state and output equations are given as follows:

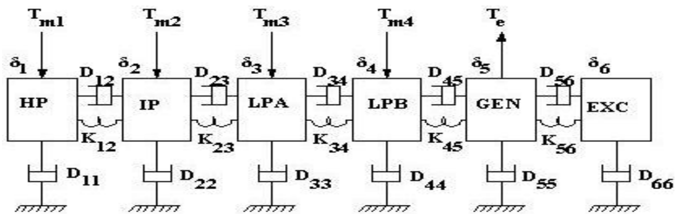

Figure 2. Six-Spring mass model of mechanical system

$$\dot{\delta}_i = \omega_i \text{ , i=1,2,3,4,5,6}$$

$$\dot{\omega}_1 = \frac{\left[-\left(D_{11}+D_{12}\right)\omega_1 + D_{12}\omega_2 - K_{12}(\delta_1-\delta_2)+T_{m1}\right]}{M_1}$$

$$\dot{\omega}_2 = \frac{\begin{bmatrix}\left(D_{12}\omega_1 - (D_{12}+D_{22}+D_{23}\right)\omega_2 + \\ D_{23}\omega_3 - K_{12}(\delta_2-\delta_1) - K_{23}(\delta_2-\delta_3)) + T_{m2}\end{bmatrix}}{M_2}$$

$$\dot{\omega}_3 = \frac{\begin{bmatrix}\left(D_{23}\omega_2 - (D_{23}+D_{33}+D_{34}\right)\omega_3 + \\ D_{34}\omega_4 - K_{23}(\delta_3-\delta_2) - K_{34}(\delta_4-\delta_3)) + T_{m3}\end{bmatrix}}{M_3} \tag{5}$$

$$\dot{\omega}_4 = \frac{\begin{bmatrix}\left(D_{34}\omega_3 - (D_{34}+D_{44}+D_{45}\right)\omega_4 + \\ D_{45}\omega_5 - K_{34}(\delta_4-\delta_3) - K_{45}(\delta_4-\delta_5)) + T_{m4}\end{bmatrix}}{M_4}$$

$$\dot{\omega}_5 = \frac{\begin{bmatrix}\left(D_{34}\omega_3 - (D_{34}+D_{44}+D_{45}\right)\omega_4 + \\ D_{45}\omega_5 - K_{34}(\delta_4-\delta_3) - K_{45}(\delta_4-\delta_5)) + T_{m4}\end{bmatrix}}{M_4}$$

$$\dot{\omega}_6 = \frac{\begin{bmatrix}\left(D_{56}\omega_5 - (D_{56}+D_{66}\right)\omega_6 \\ + D_{56}\omega_6 - K_{56}(\delta_6-\delta_5)) + T_e\end{bmatrix}}{M_6}$$

After linearzing the above equations the state and output equations can be written as:

$$\dot{X}_M = A_M X_M + B_{M1}U_{M1} + B_{M2}U_{M2} \tag{6}$$

$$Y_M = C_M X_M \tag{7}$$

$$X_M = \left[\Delta\delta_1, \Delta\delta_2, \Delta\delta_3, \Delta\delta_4, \Delta\delta_5, \Delta\delta_6, \Delta\omega_1, \Delta\omega_2, \Delta\omega_3, \Delta\omega_4, \Delta\omega_5, \Delta\omega_6\right]^t, \ Y_M = \left[\Delta\delta_5, \Delta\omega_5\right]^t,$$

$$U_{M1} = \left[\Delta I_D, \Delta I_Q\right]^t, \ U_{M2} = \left[\Delta i_D, \Delta i_Q\right]^t$$

C. Excitation system

The state and output equations of the linearized IEEE type 1 exication system model are derived as

$$\dot{X}_E = A_E X_E + B_E U_E \tag{8}$$

$$Y_E = C_E X_E$$

Where $X_R = [\Delta V_f \quad \Delta V_s \quad \Delta V_{gr}]^t$, $Y_E = \left[\Delta V_t\right]$, $U_E = \left[\Delta V_g\right]$

D. Network

The transmission line (Figure 3) is represented by lumped parameter T- circuit. The network has been represented by its α–axis equivalent circuit, which is identical with the positive sequence network.

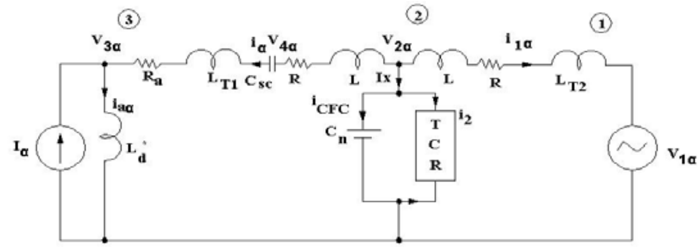

Figure 3. α– axis representation of the network

$$(L+L_{T2})\frac{di_{1\alpha}}{dt}=V_{2\alpha}-V_{1\alpha}-Ri_{1\alpha}$$

$$(L+L_{A})\frac{di_{\alpha}}{dt}=V_{2\alpha}-(R+R_{A})i_{\alpha}-L''_{d}\dot{I}_{\alpha}-V_{4\alpha}$$

$$C_{n}\frac{dV_{2\alpha}}{dt}=-i_{2\alpha}-i_{\alpha}-i_{1\alpha}$$

$$C_{se}\frac{dV_{4\alpha}}{dt}=-i_{\alpha} \tag{9}$$

where $L_A = L_{T1} + L''_d$ and $C_n = C + C_{FC}$

Similarly, the equations can be derived for the β- network. The α-β network equations are then transformed to D-Q frame of reference and subsequently linearised. The state and output equations for the network model are finally obtained as:

$$\dot{X}_N = [A_N]X_N + [B_{N1}]U_{N1} + [B_{N2}]U_{N2} + [B_{N3}]U_{N3} \tag{10}$$

$$Y_{N1} = [C_{N1}]X_N + [D_{N1}]U_{N1} + [D_{N2}]U_{N2} + [D_{N3}]U_{N3}$$

$$Y_{N2} = [C_{N2}]X_N,\ Y_{N3} = [C_{N3}]X_N$$

Where,

$$X_N = [\Delta i_{1D}\ \Delta i_D\ \Delta v_{2D}\ \Delta v_{4D}\ \Delta i_{1Q}\ \Delta i_Q\ \Delta v_{2Q}\ \Delta v_{4Q}\ ]^t$$

$U_{N1} = [\Delta i_{2D}\ \ \Delta i_{2Q}\ ]^t$, $U_{N2} = [\ \Delta\dot{I}_D\ \ \Delta\dot{I}_Q\ ]^t$ and $U_{N3} = [\ \Delta I_D\ \ \Delta I_Q\ ]^t$

$Y_{N1} = [\Delta V_{gD}\ \ \Delta V_{gQ}]^t$, $Y_{N2} = [\Delta i_D\ \ \Delta i_Q]^t$ and $Y_{N3} = [\Delta V_{2D}\ \ \Delta V_{2Q}]^t$

E. Static Var System

Figure. 4 shows a small signal model of a general SVS. The terminal voltage perturbation ΔV and the SVS incremental current weighted by the factor K_D representing current droop are fed to the reference junction. T_M represents the measurement time constant, which for simplicity is assumed to be equal for both voltage and current measurements. The voltage regulator is assumed to be a proportional- integral (PI) controller. Thyristor control action is represented by an average dead time T_D and a firing delay time T_s. ΔB is the variation in TCR susceptance. ΔV_F represents the incremental auxiliary control signal.

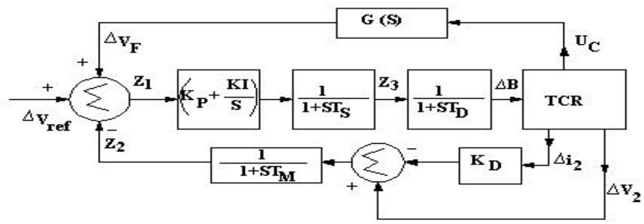

Figure 4. SVS control system with auxiliary feedback

$$L_S \frac{di_{2\alpha}}{dt} = V_{2\alpha} - R_S i_{2\alpha}$$

$$L_S \frac{di_{2\beta}}{dt} = V_{2\beta} - R_S i_{2\beta} \tag{11}$$

Where R_S, L_S represent TCR resistance and inductances respectively. The other equations describing the SVS model are:

$$\dot{z}_1 = V_{ref} - z_2 + \Delta V_F$$

$$\dot{z}_2 = \frac{(\Delta V_2 - K_D \Delta i_2)}{T_M} - \frac{z_2}{T_M}$$

$$\dot{z}_3 = \frac{(-K_I z_1 + K_P z_2 - z_3 - K_P \Delta V_{ref})}{T_s}$$

$$\Delta\dot{B} = \frac{(z_3 - \Delta B)}{T_D}$$

Where ΔV_2, Δi_2 are incremental magnitudes of SVS voltage and current, respectively, obtained by linearising

$$V_2 = \sqrt{(V_{2D}^2 + V_{2Q}^2)}\ ,\ i_2 = \sqrt{(i_{2D}^2 + i_{2Q}^2)}$$

The state and output eqns. of the SVS model are obtained as:

$$\dot{X}_S = [A_S]X_S + [B_{S1}]U_{S1} + [B_{S2}]U_{S2} + [B_{S3}]U_{S3} \tag{12}$$

$$Y_S = [C_S]X_S + [D_S]U_{S1}$$

Where

$$X_S = [i_{2D} \quad i_{2Q} \quad Z_1 \quad Z_2 \quad Z_3 \quad \Delta B]^t,\ U_{S1} = [\Delta V_{2D} \quad \Delta V_{2Q}]^t,\ U_{S2} = \Delta V_{REF},$$

$$U_{S3} = \Delta V_F \ \&\ Y_S = [\Delta i_{2D} \quad \Delta i_{2Q}]^t$$

3. Auxilary Controller

A. Combined Derivative of Reactive Power and Derivative of Computed Internal Voltage (CDRPDCIV) Auxiliary Controller

The auxiliary controller signal in this case is the combination of derivative of the line reactive power and the derivative of computed internal voltage with the objective of utilizing the beneficial contribution of both signals towards improving the dynamic performance of the system. The control scheme for the composite controller is illustrated in Figure.5. The auxiliary control signals U_{C1} and U_{C2} correspond, respectively, to the derivative of line reactive power and the derivative of computed internal voltage deviations which are derived at the SVS bus.

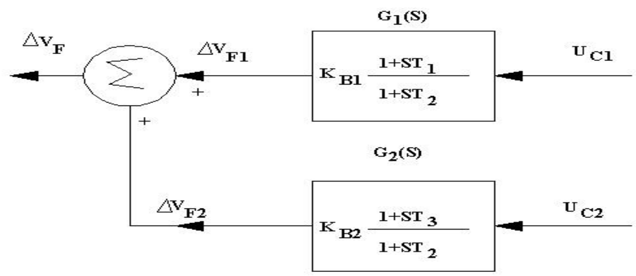

Figure 5. Control scheme for (CDR.PDCIV) auxiliary controller

1). *Derivatie of Reactive Power Auxiliary Signal*

The auxiliary control signal in this case is the deviation in the line reactive power entering the SVS bus. The reactive power entering the SVS bus can be expressed as:

$$Q_2 = V_{2D} i_Q - V_{2Q} i_D \tag{13}$$

where i_D , i_Q and V_{2D}, V_{2Q} are the D-Q axis components of the line current i and the SVS bus voltage V_2 respectively. Linearizing eqn. (13) gives the deviation in the reactive power as:

$$\Delta Q_2 = V_{2D_O}\Delta i_Q + i_{Q_O}\Delta V_{2D} - V_{2Q_O}\Delta i_D - i_{D_O}\Delta V_{2Q} \tag{14}$$

$$\Delta Q_2 = [F_6]X_T \tag{15}$$

where F_6= (1x33) vector having non zero elements as

$F_6(1,21)=V_{2Qo}$, $F_6(1,25)=-V_{2Do}$,$F_6(1,22)=-i_{Qo}$,$F_6(1,26)=i_{Do}$

The derivative of the reactive power is obtained by differentiating eq. (10)

$$\Delta\dot{Q}_2 = F_6[AX_T + BU_{S3}] = [F_7]X_T \tag{16}$$

where $F_7 = F_6A$ and $F_6B=0$

The equation (16) can be written as

$U_{C1} = [F_{CR}]X_R+[F_{CM}]X_M+[F_{CE}]X_E+ [F_{CMN}]X_N+[F_{CS}]X_S$

where $U_{c1} = \Delta\dot{Q}_2$

2). Derivative of Computed Internal Voltage Auxiliary Signal

The derivative of computed internal voltage signal has been derived by computation of internal voltage of the remotely located generator utilizing locally measurable SVS bus voltage and transmission line currents. The DCIV signal has a more beneficial influence on the high frequency Torsional oscillations. As it is not feasible to obtain this signal by measurement as the generating station and the SVS are located far apart from each other, therefore it is attempted to derive the proposed signal in terms of parameters, which are available at SVS bus. The parameters utilized for the signal are bus voltage, transmission line current at SVS bus and reactance between the generator and SVS terminal. The line charging capacitance and the resistance of the generator stator and the transmission line are neglected. The dependent current source represent the generator and transformed to an equivalent voltage source behind the sub-transient inductance, From the equivalent circuit, the total inductance L_E between the bus and equivalent source e_1 is given as:

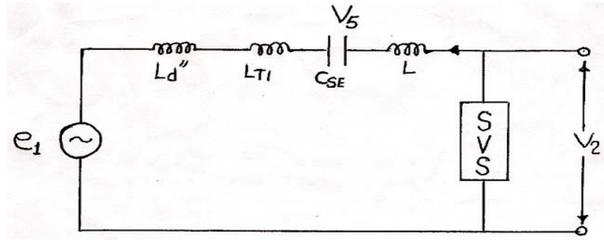

Figure 6. α-axis representation of simplified system for DCIV signal

$$L_E = L_d{}'' + L_{T1} + (X_L - X_C)/\omega_0$$

The α and β axis component of internal voltage e_1 are expressed as:

$$e_{1\alpha} = V_{2\alpha} + L_E \frac{d_{i\alpha}}{dt} - V_{5\alpha} \tag{17}$$

$$e_{1\beta} = V_{2\beta} + L_E \frac{d_{i\beta}}{dt} - V_{5\beta} \tag{18}$$

The above equations are transformed to D-Q frame of reference as:

$$e_{1D} = V_{2D} + L_E\, i_D + \omega_0\, L_E i_Q - V_{5D} \tag{19}$$

$$e_{1Q} = V_{2Q} + L_E\, i_Q + \omega_0\, L_E i_D - V_{5Q} \tag{20}$$

where e_{1D} and e_{1Q} are D-Q axis component of the internal voltage e_1 respectively.

The computed internal voltage signal is obtained as:

$$e_1^2 = e_{1q}^2 + e_{1d}^2 \tag{21}$$

After linearising equation (21)

$$\Delta e_1 = \frac{1}{e_{10}}\left[e_{1D0}\Delta e_{1D} + e_{1Q0}\Delta e_{1Q} \right] \tag{22}$$

Putting the value of Δe_{1D} and Δe_{1Q} in equation (22):

$$\Delta e_1 = \frac{e_{1D0}}{e_{10}}\left[\Delta V_{2D} + L_E\, \Delta\dot{i}_D + \omega_0 L_E \Delta i_Q - \Delta V_{5D}\right] +$$

$$\frac{e_{1Q0}}{e_{10}}\left[\Delta V_{2Q} + L_E\, \Delta\dot{i}_Q + \omega_0 L_E \Delta i_D - \Delta V_{5Q}\right]$$

$$\Delta e_1 = [F_1]X_T + .[F_2]\dot{X}_T \tag{23}$$

Where $X_T = [X_R X_M X_E X_N X_S]$

$F_1 = (1 X 35)$ Vector having non-zero element as follows:

$$F_1(1,21)=\frac{e_{1Q0}}{e_{10}}\omega_0 L_E,\ F_1(1,22)=\frac{e_{1D0}}{e_{10}}\ F_1(1,23)=-\frac{e_{1D0}}{e_{10}}$$

$$F_1(1,25)=\frac{e_{1D0}}{e_{10}}\omega_0 L_E,\ F_1(1,26)=\frac{e_{1Q0}}{e_{10}},\ F_1(1,27)=-\frac{e_{1Q0}}{e_{10}}$$

$$F_2(1,21)=\frac{e_{1D0}}{e_{10}}L_E,\ F_2(1,25)=\frac{e_{1Q0}}{e_{10}}L_E$$

$\dot{X}_T = AX_T + BU_{S3}$ in equation

$$\Delta e_1 = F_1[X_T] + F_2[AX_T + BU_{S3}] \tag{24}$$

$$\Delta e_1 = [F_3]X_T,\ \text{where}\ F_3 = [F_1 + F_2 A]\ \text{and} \tag{25}$$

$F_2B = 0$

The derivative of computed internal voltage is given as:

$\Delta\dot{e}_1 = [F_3]\dot{X}_T$

After expanding the equation (25)

$U_{C2} = [F_{CR}]X_R+[F_{CM}]X_M+[F_{CE}]X_E+ [F_{CMN}]X_N+[F_{CS}]X_S$

Where $UC_2 = \Delta\dot{e}_1$

The state and output equations of the different constituent subsystems along with the auxiliary controller state and output equations are combined to result in the linearised state equations of overall system as:

$$\dot{X}_T = [A]X \tag{26}$$

where, $X_T = [\ X_R \quad X_M \quad X_E \quad X_N \quad X_S \quad X_C\ ]^t$.

The dimension of the system matrix is 35

4. The Controlled Series Compensation (Csc) Scheme

The CSC scheme as shown in Figure 7 has been simulated by step wise control of the degree of series compensation by means of sections with thyristor by pass switches. The scheme is implemented as follows.

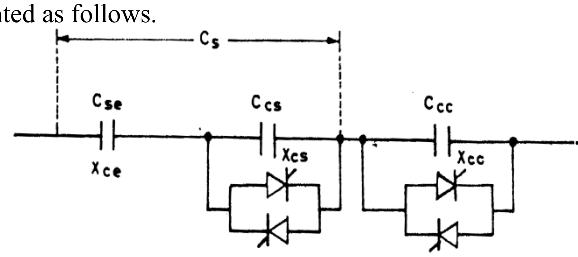

Figure 7. Controlled series compensation scheme

The series capacitor C_s of the line is split into two segments C_{se} and C_{cs} with capacitive reactances X_{ce} and X_{cs} respectively. C_{se} is left as permanent series compensation while C_{cs} is made controllable segment. Another capacitor segment C_{cc} equal in magnitude to that of C_{cs}, and having capacitive reactance X_{cc} is also added in series with the line. During steady state condition the capacitor segment remains by passed. For the damping purpose using series arrangement the reactance $\pm X_{cs}$/ph is selected. Two X_{cs}/ph capacitor segments are connected in series with the line. In steady state one capacitor segment is bypassed and other one remains in operation. The controlled capacitive reactance 'X_{ccap}' can be defined as:

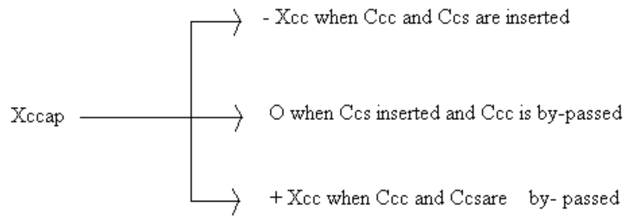

The control algorithm used senses the angular speed deviations from the steady state value and increases or decreases the power transmission by inserting on by passing the controlled series capacitors when angular speed deviations ($\Delta\omega$) reaches a threshold value of $+\Delta\omega_{Th}$ or $-\Delta\omega_{Th}$ rad/sec respectively. Otherwise the controlled series capacitor C_{cc} remain by -passed. A threshold value of $\Delta\omega_{Th}$ (0.14 rad/sec) is used to prevent the damping system from sustained continuous operation. In such a way the full bang-bang control characteristics of the CSC is obtained. The value of $\Delta\omega_{Th}$ can be adjusted to minimize the frequent switching of the controlled series capacitor so that the voltage transients are reduced.

5. Case Study

The study system consists of 1110 MVA synchronous generator supplying power to an infinite bus over a 400 kV, 600 km. long series compensated single circuit transmission line. The system data and torsional spring mass system data are given in Appendix A. The SVS rating for the line has been chosen to be 100 MVAR inductive to 300 MVAR capacitive. 25%, 40% and 48% series compensation is used at the sending end of the transmission line.

A . Torsional Oscillations Study

The eigen values have been computed for the system with and without (DCRPDCIV) auxiliary controller incorporated in SVS control system for wide range of series compensation at higher power transfer level. Table1 presents the eigen values for the system at generator power P_G= 800 MW for compensation levels of 25%, 40% and 48% without any auxiliary controller. When no auxiliary controller is incorporated., Mode 4 and 5 are unstable for all levels of series compensation used. Mode3 is unstable at 48% and mode2 is unstable at 25%. Mode1 is unstable at 25% and 48%. Mode 2 is unstable at 25% and Mode0 is unstable at 25% and 40% level of series compensation in the system at P_G= 800 MW.

Table 1. System Eigen Values Without Auxilary Controller PG=800MW

MODE	S=25%	S=40%	S=48%
MODE 5	.0000±j298.1005	.0000±j298.1005	.0001±j298.1005
MODE 4	.1113±j202.7263	.0487±j202.9565	.0294±j202.7049
MODE 3	-.0090±j160.5242	-.0062±j160.5301	.1803±j160.6361
MODE 2	.0032±j126.9691	-.0020±j126.9767	-.0011±j126.9919
MODE 1	.0100±j98.7329	-.0171±j98.8552	.0328±j98.6392
MODE 0	.0151±j4.9875	.2480±j4.9116	-.5786±j7.8136
ELECTRICAL MODE	-10.4268±j192.6662	-9.0660±214.6401	-13.2924±168.8582

Table 2 shows the system Eigen value when combined derivative of Reactive power and derivative of Computed internal Voltage Auxiliary Controller is incorporated in SVS control system. It can be seen that all the modes are stable at P_G = 800 MW for all levels of series compensation. Table3 presents the eigen values for the system at generator power P_G= 200,500 and 800 MW for compensation level of 15% without any auxiliary controller. When no auxiliary controller is incorporated, Modes 5, 4, 3 are unstable at all power transfer levels and Modes 1and 0 are unstable at PG=800MW.

Table 2. System Eigen Values With Derivative Of Reactive Power And Derivative Computed Internal Voltage Auxiliary Controller PG=800MW

MODE	S=25% K_{B1}=-0.0006 T_1=0.009 T_2=0.5 K_{B2}=- 0.00005 T_3=0.003T_4=0.2	S=40% K_{B1}=-.014, T_1=0.01, T_2=0.065 K_{B2}=- 0.0004, T_3=0.003, T4=0.2	S = 48% K_{B1}=-.001, T_1=.01, T_2=0.1 K_{B2}=-.0029, T_3=0.003, T_4=0.3
MODE 5	-.0007±j298.1006	-.0001±j298.1004	-.0210±j298.1003
MODE 4	-.1365±j202.7224	-.0041±j203.0146	-.0165±j202.6959
MODE 3	-.0269±j160.5244	-.0115±j160.5290	-.0037±j160.6427
MODE 2	-.0187±j126.9689	-.0025±j126.9764	-.0053±j126.9856
MODE 1	-.0024±j98.7304	-.0232±j98.8576	-.1176±j98.5868
MODE 0	-.1047±5.0314	-.7574±j3.6808	-.9007±j7.9986
ELECTRICAL MODE	-10.3878±192.7277	-3.7849±213.1617	-12.7568±173.9231

Table 4 shows the system eigen values when combined derivative of Reactive power and derivative of Computed internal Voltage Auxiliary Controller is incorporated in SVS control system. It can be seen that all the modes are stable at all levels of power transfer at 15% of series compensation The auxiliary controller parameter are selected based on an extensive root locus study and are listed in Table 2 and 4.

Table 3. System Eigen Values Without Auxilliary Controller

MODE	P_G = 200 MW	P_G = 500 MW	P_G = 800 MW
MODE 5	.0000±j298.1006	.0000±j298.1006	.0000±j298.1006
MODE 4	.0593±j202.7368	.0681±j202.7265	.1118±j202.7264
MODE 3	.0111±j160.5519	.0050±j160.5464	-.0089±j160.5241
MODE 2	-.0008±j126.9794	-.0017±j126.9764	-.0032±j126.9691
MODE 1	-.0167±j98.8784	-.0090±j98.8381	.0100±j98.7327
MODE 0	-.3969±j4.7451	-.1985±j5.0264	.0153±j4.9871
ELECTRICAL MODE	-9.564±j189.3292	-9.5753±j188.8829	-10.4269±j192.6654

Table 4. System Eigen Values with Combined Derivative of Computed Internal Voltage & Derivative of Reactive Power with Imdu at 15% Compensation Level

MODE	PG=200MW K_{B1}=-0.0095, T_1=0.01, T_2=0.065 K_{B2}=- 0.0001, T_3=0.003 T_4=0.05	PG=500MW K_{B1}=-0.007, T_1=0.03, T_2=0.065 K_{B2}=- 0.0001, T_3=0.002, T_4=0.07	PG=800MW K_{B1}=-.006, T_1=0.01, T_2=0.065 K_{B2}=-0 .00009, T_3=0.003, T_4=0.095
MODE 5	-.0021±j298.1003	-.0001±j298.1001	-.0001±j298.1003
MODE 4	-.0602±j202.9976	-.1118±j202.9416	-.2232±j203.3566
MODE 3	-.0275±j160.5462	-.0376±j160.5324	-.0755±j160.5956
MODE 2	-.0025±j126.9811	-.0052±j126.9793	-.0101±j126.9886
MODE 1	-.0254±j98.9306	-.0160±j98.9368	-.0044±j99.0772
MODE 0	-.8161±j5.3236	-.7406±j6.6827	-.9448±j7.2488
ELECTRICAL MODE	-.8464± j232.3454	-.8026± j235.9512	-.0019 ±j219.5462

B. Time Domain Simulation Study

A The transient simulation of the combined non linear system including CDRPDCIV SVS Auxiliary controller and controlled series compensation has been carried out to illustrate the effectiveness of the CDRPDCIV auxiliary controller in coordination with CSC under large disturbance conditions for damping power oscillations. Applying a pulsed torque of 20% for 0.1s simulates a disturbance. The simulation study has been carried out at P_G=800MW for 40% series compensation level. All the self and mutual damping constants are assumed to be zero.

Figure 8(a-g) shows the time response curves of the terminal voltage, SVS bus voltage, SVS susceptance, power angle, variation in torsional torques T(HP-IP), T(LPB-Generator) without CDRPDCIV auxiliary controller after the disturbance respectively which are obtained by solving non linear differential equations of the generator, network, Static var system and mechanical system as given in Appendix using Runge-Kutta Fourth order method. It can be seen from the Figure 8 that there are sustained oscillations in voltage, power angle and deviation in rotor angular speed. This is due to the instability of mode 0 (System mode) as is evident in eigen value study (Table 1). Mode 0 instability is caused by controller interaction with the network and generator electrical quantities. Torsional torques oscillations start growing almost as soon as disturbance is applied. This is due to the instability of torsionsal modes 5 and 4 which corroborate the results of eigen value study.

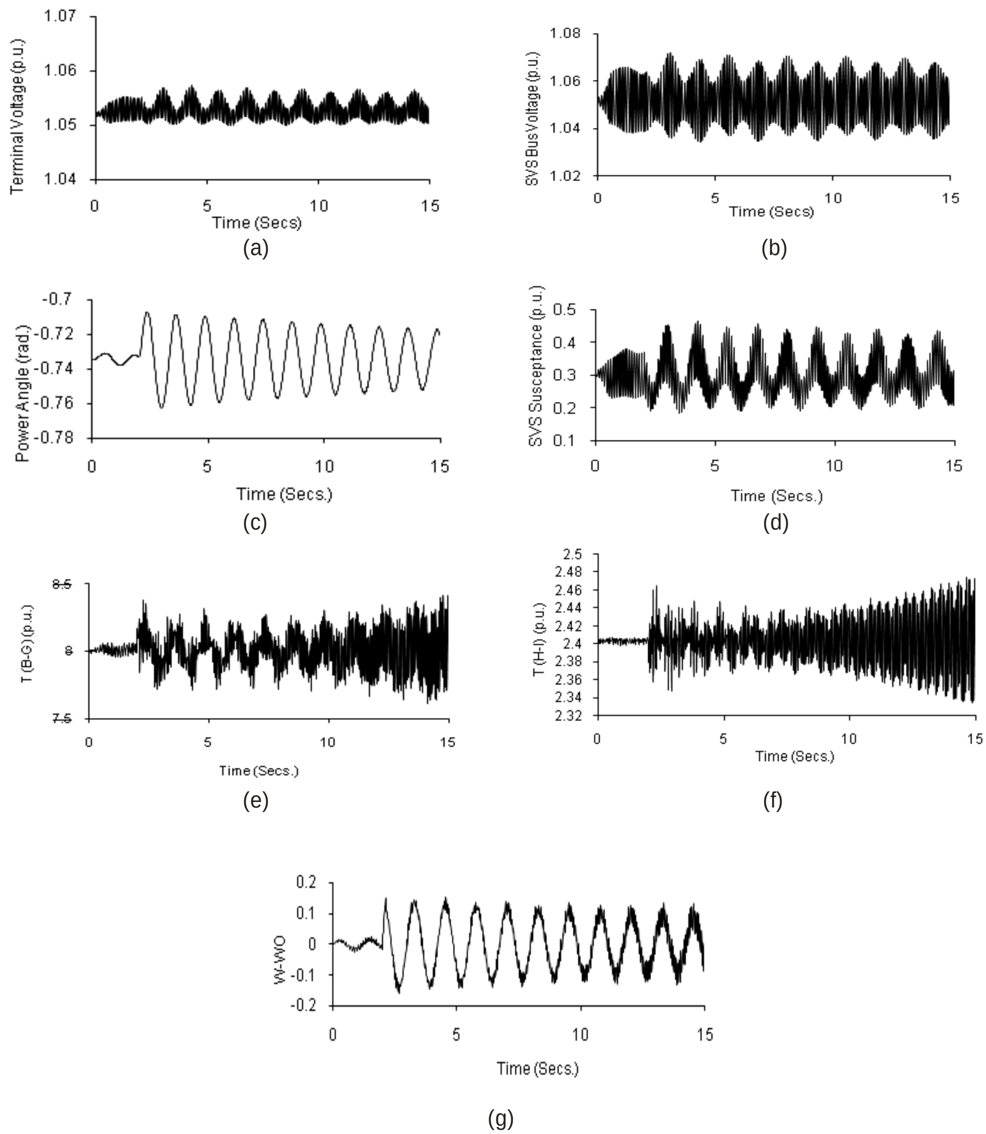

Figure 8(a-g). Response curves without CDRPDCIV auxiliary controller at Pg = 800 MW due to 20% increase in T_{mech} for 0.1 secs (T-circuit Model)

Figure 9(a-g). Shows the response curves of the terminal voltage, SVS bus voltage, SVS susceptance, power angle, variation in torsional torques T(HP-IP), T(LPB-Generator) respectively with CDRPDCIV auxiliary controller after the disturbance which are obtained by solving non linear differential equations of the system using Runge Kutta Fourth order method. It is seen that CDRPDCIV auxiliary controller damps out voltage, power angle and torsional torques oscillations by modulating reactive and active power of the system.

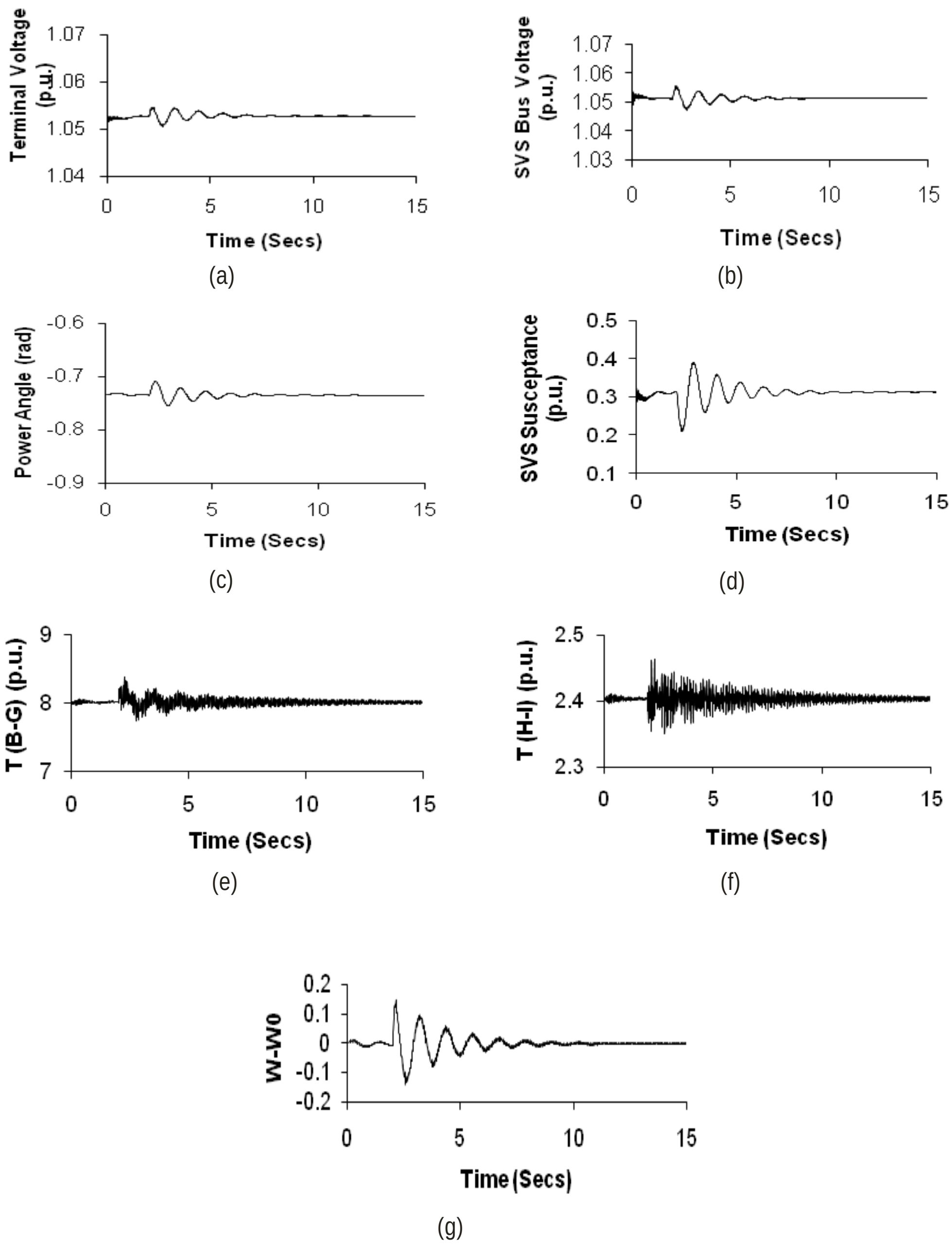

Figure 9(a-g). Response curves with CDRPDCIV auxiliary controller at Pg = 800 MW due to 20% increase in T_{mech} for 0.1 secs (T-circuit Model)

Figure 10(a-h) shows the response curves of the terminal voltage, SVS bus voltage, SVS susceptance, power angle, variation in controlled capacitive reactance variation in torsional torques with the CDRPDCIV auxiliary controller in coordination with CSC after the disturbance. It is seen that the coordinated application of CDRPDCIV auxiliary controller and CSC damps out voltage , power angle and torsional torques oscillations effectively and settling time is considerably reduced and a significant improvement in dynamic and transient performance is achieved.

The bang-bang control characteristics of the CSC give rise to voltage transients. The voltage transients are controlled by closely restricting the reactive power limits of the SVS (0 to 0.4 pu in the present case) and avoiding the frequent switching of controlled capacitor.

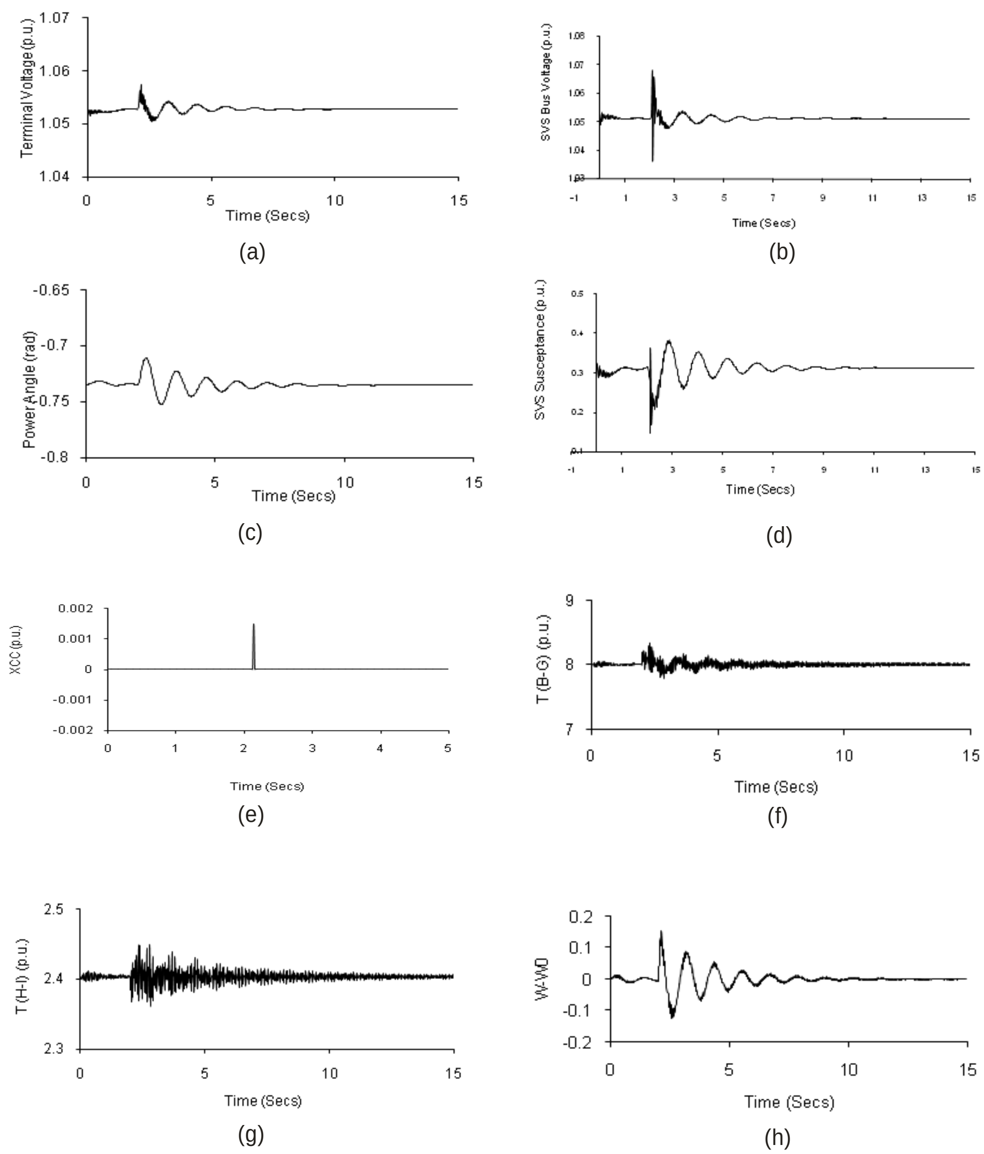

Figure 10(a-h). Response curves with CDRPDCIV auxiliary controller and controlled series compensation at Pg = 800 MW due to 20% increase in T_{mech} for 0.1 secs (T-circuit Model)

Conclusion

In this paper the effectiveness of coordinated application of CSC and DRPDCIV auxiliary controller has been evaluated for damping power oscillations for a series compensated power system over a wide operating range of power transfer. The following conclusions can be drawn from the eigenvalue and time domain simulation study performed.

1. The proposed SVS auxiliary controller can stabilize all the torsional modes for wide range of series compensation and power transfer levels.
2. CSC in coordination with DRPDCIV auxiliary controller developed for SVS rapidly damps out the voltage, power angle and torsional oscillations thus enhancing the dynamic and transient performance of system..
3. CSC generates the voltage transients with its bang- bang form of control. These voltage transients can be controlled by restricting the reactive power limits of SVS and its frequent switching. Thus the proposed damping controller provides an efficient and robust control of power oscillations damping over a wide operating range and under large disturbance conditions.

Nomenclature

C_{FC}	Fixed Capacitance of SVS branch
C_{sc}	Series Capacitance and C_n=C_{FC}+C
K_B	Gain of SVS Auxiliary Controller
I_α	α-axis current of synchronous machine
K_D	Slope of SVS control characteristics
K_I	Integral gain of SVS voltage controller
K_P	Proportional gain of SVS voltage controller
L_d''	Subtransient inductance of synchronous machine
Te	Electrical Torque, T_m= Mechanical Torque
T_d	Thyristor dead time constant
T_M	Measurement time constant
T_S	Firing delay constant
V_F	Auxiliary control signal
Δ	Power angle,
θ	Bus angle,
ψ	Flux linkage

References

[1] Balda J.C. Eitelberg E. and Harley R.G., "Optimal output Feedback Design of Shunt Reactor Controller for Damping Torsional Oscillations", *Electric Power System research* Vol.10 1986, pp 25-33.

[2] Einar V. Larsen, Juan J. Sanchez-Gasca and Joe H. chow,"Concepts for design of FACTS controllers to damp power swings," *IEEE Trans. On Power Systems*, Vol 10, No.2pp 948-956, May 1995.

[3] James F. Gronquist, William A. Fernando L. Alvardo and Robert H. Lasseter," Power oscillation damping control strategies for ACTS devices using locally measurable quantities," *IEEE Trans. On Power Systems*, Vol 10, No 3, pp 1598-1605, August 1995.

[4] Narendra Kumar, M.P. Dave, "Application of auxiliary controlled static var system for damping sub synchronous resonance in power systems. *Electric Power System Research* 37 (1996) 189 – 201.

[5] X Chen, N. Pahalawaththa, U. Annakkage, C. Kumble, " Controlled series compensation for improving stability of multimachine power systems, *IEE Proc.*142 (Pt.C) (1995) 361-366

[6] Noroozian, M. Ghandhari, M. Andersson,G. Gronquist J. Hiskens, "A robust control strategy for shunt and series reactive compensators to damp electromechanical oscillations" *IEEE Trans. On Power Delivery*, Vol.16, Oct (2001) 812-817.

[7] N. Pillai, Arindam Gosh, A. Joshi, "Torsional Oscillation Studies in an SSSC Compensated Power System", *Electric Power System research* 55(2000)57-64.
[8] Ning, Yang, Q. Liu, J. D. McCalley, "TCSC controller Design for Damping Inter Area Oscillations", *IEEE Trans. On Power System*, 3(4) (1998) 1304-1310.
[9] R.S. Ramshaw, K.R. Padiyar, "Generalized system Model for Slip Ring Machines", *IEEE Proc*.120 (6) 1973.
[10] K. R. Padiayar, R.K. Varma, "Damping Torque Analysis of Static Var Controllers", *IEEE Trans. on Power Systems*, 6(2) (1991) 458-465.
[11] J. Chen, T.T. Lie and D.M. Vilathgamuwa , "Enhancement of power system damping using VSC-based series connected FACTS controllers" *IEE Proc.-Gener. Transm. Distrib...* Vol. „150, No. 3, May2003, pp 353-359
[12] Januszewski, M. Machowski, J Bialek J.W.,"Application of direct Lyapunov method to improve damping of power swings by control of UPFC, *IEE Proc. Genr. Trans. Distrib*. vol 151, (2004), 252-260.
[13] Chaudhuri, B. Pal, B.C. "Robust damping of multiple swing modes employing global stabilizing signals with TCSC", *IEEE Trans. On Power Syst*., Vol.19, pp. 499-506, Feb.2004.
[14] Massimo Bongiorno, Jan Svensson, Lennart Angquist, "Single–Phase VSC Based SSSC for Sub synchronous Resonance Damping," *IEEE Trans. On Power Delivery*, Vol. 23, July 2008, 1544-1550.
[15] S. K. Gupta and Narendra Kumar, "Controlled Series Compensation in coordination with double Order SVS Auxiliary Controller and Inductiopn Machine for repressing the Torsional Oscillations in Power system". *Electric Power System Research* 62(2002) 93-103.
[16] Rajiv K.Varma, Soubhik Auddy and Ysni Semsedini, "Mitigation of sub synchronous resonance in a series-compensated wind farm using FACTS controllers", *IEEE transactions on power delivery*, vol. 23, no. 3, pp. 1645-1654, 2008.
[17] Alberto Mota Simões, Diego Chaves Savelli, Paulo César Pellanda, Nelson Martin and Pierre Apkarian, "Robust Design of a TCSC Oscillation Damping Controller in a Weak 500-kV Interconnection Considering Multiple Power Flow Scenarios and External Disturbances", *IEEE transactions on power systems*, vol. 24, no. 1, pp.226-236, 2009

Appendix A

Generator data: 1110MVA, 22kV

$R_a = 0.0036$, $X_L = 0.21$ $T'_{do} = 6.66$, $T'_{qo} = 0.44$, $T''_{do} = 0.032$, $T''_{qo} = 0.057s$ $X_d = 1.933$, $X_q = 1.743$,

$X'_d = 0.467$, $X'_q = 1.144$,

$X''_d = 0.312$, $X''_q = 0.312$ p.u.

IEEE type 1 excitation system:

$T_R=0$, $T_A=0.02$, TE=1.0, TF=1.0s, $K_A=400$, $K_E=1.0$; $K_F=0.06$ p.u. $V_{Fmax}=3.9$, $V_{Fmin}=0$, $V_{Rmax}=7.3$, $V_{R\,min}=-7.3$

Transformer data:

$R_T=0$, $X_T=0.15$ p.u. (generator base)

Transmission line data:

Voltage 400kV, Length 600km, Resistance R=0.034Ω / km, Reactance X=0.325 Ω / km, Susceptance $B_c=3.7\mu$ mho / km

SVS data: Six-pulse operation:

$T_M=2.4$, $T_S=5$, $T_D = 1.667ms$, $K_I = 1200$, $K_P = 0.5$, $K_D = 0.01$

Governing equations of system

$$V_{gD} = R_a i_D + L''_D\left(\dot{i}_D + \dot{I}_D\right) + \omega_o L''_D\left(i_q + I_Q\right)$$

$$V_{gQ} = R_a i_q + L''_D\left(\dot{i}_q + \dot{I}_Q\right) - \omega_o L''_D\left(i_D + I_D\right)$$

$V_g = \sqrt{V_{gD}^2 + V_{gQ}^2}$ =Generator Terminal Voltage

$$V_{2D} = L_s\left(\dot{i}_{2D} + \omega_o i_{2Q}\right) + R_s i_{2D}$$

$$V_{2Q} = L_s\left(\dot{i}_{2Q} - \omega_o i_{2D}\right) + R_s i_{2Q}$$

$V_2 = \sqrt{V_{2D}^2 + V_{2Q}^2}$ =SVS bus voltage

$\Delta\dot{B} = \dfrac{(z_3 - \Delta B)}{T_D}$ =SVS susceptance

$$\dot{z}_1 = V_{ref} - z_2 + \Delta V_F$$

$$\dot{z}_2 = \frac{(\Delta V_2 - K_D \Delta i_2)}{T_M} - \frac{z_2}{T_M}$$

$$\dot{z}_3 = \frac{(-K_I z_1 + K_P z_2 - z_3 - K_P \Delta V_{ref})}{T_s}$$

$T(H-I) = K_{12}\left(T_{m1} - T_{m2}\right)$=Section torque between high pressure and intermediate pressure turbine

$T(LPB-G) = K_{45}\left(T_{m4} - T_{m5}\right)$ where T_{m1}, T_{m2}, T_{m3} and T_{m4} have been derived from eq.(5) of mechanical system.

Torsional spring-mass system data

Mass	Shaft	Inertia H(s)	Spring constant K (p.u. Torque/rad.)
HP		0.1033586	
	HP-IP		25.772
IP		0.1731106	
	IP-LPA		46.635
LPA		0.9553691	
	LPA-LPB		69.478
LPB		0.9837909	
	LPB-GEN		94.605
GEN		0.9663006	
	GEN-EXC		3.768
EXC		0.0380697	

All self and mutual damping constants are assumed to zero.

P. R. Sharma was born in 1966 in India. He is currently working as Associate Professor in Electrical Engg. in the department of Electrical and Electronics Engineering in YMCA University of Science & Technology, Faridabad. He received his B.E Electrical Engineering in 1988 from Punjab University Chandigarh, M.Tech in Electrical Engineering (Power System) from Regional Engineering College Kurukshetra in 1990 and Ph.D from M.D.University Rohtak in 2005. He started his carrier from industry. He has vast experience in the industry and teaching. His area of interest is Optical location and coordinated control of FACTS devices.